CONTROLLED LROC NARROW ANGLE CAMERA HIGH RESOLUTION MOSAICS. S. M. Klem[1], M. R. Henriksen[1], J. Stopar[1], A. Boyd, M. S. Robinson[1], and the LROC Science Team[1], [1]School of Earth and Space Exploration, Arizona State University, Tempe, AZ 85251, USA. (sklem@ser.asu.edu)

Introduction: Controlled mosaics from Lunar Reconnaissance Orbiter Camera (LROC) Narrow Angle Camera (NAC) [1] image sequences provide an accurate cartographic framework for a host of scientific and engineering studies. Mosaics are composed of overlapping images acquired over time or from sets of images targeted across sequential orbits. NAC image pairs are first tied to an existing controlled map product: either a NAC Digital Terrain Model (DTM) [2] or an existing controlled mosaic of the area. If there is neither a DTM nor a controlled mosaic available for the area, a different pair of NAC images that have Lunar Orbiter Laser Altimeter (LOLA) cross-over smithed Spacecraft Position Kernels (SPKs) [3] are used. The images are map projected on a pixel-by-pixel basis to the WAC GLD100 [4] for a shape model. After the NAC images for the new controlled mosaic are tied to the best existing ground control, they are mosaicked together.

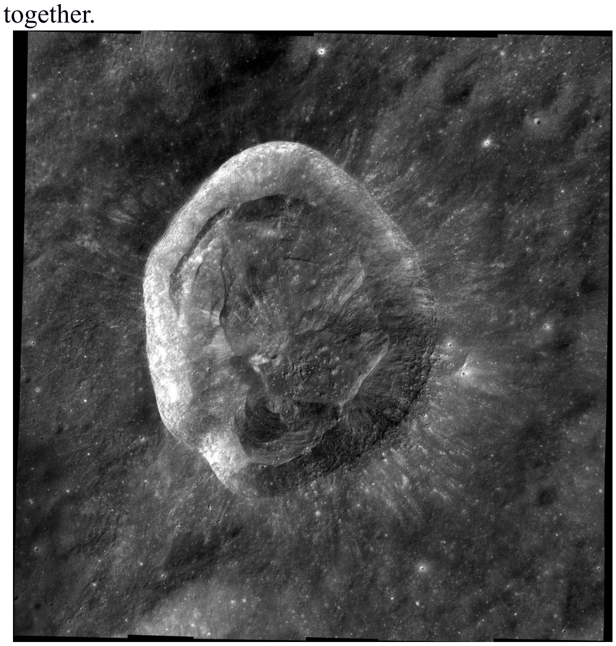

Figure 1: Larmor Q low-Sun controlled NAC mosaic (B) 1.3 m/pix constructed from three NAC pairs, total width is ~57 km, north is up.

While it is possible to make geometrically seamless mosaics using images acquired at different times and with different pixel scales, there are inevitably small photometric differences that lead to noticeable reflectance boundaries. Mosaics from NAC images acquired during non-sequential orbits have a range of incidence angles, resolution and sometimes, opposite Sun azimuths. These mosaics can also be more challenging to control. Many of the controlled mosaics are made from image sets specifically targeted (termed “Featured Mosaics” or FMs) across sequential orbits so that the lighting conditions and pixel scales are nearly invariant. Often the images that make up FMs are acquired nadir looking in the center, and slewed (from 3° to 30° degrees) moving outward. The number of NAC pairs in FMs acquired to date range from two NAC pairs to 37 NAC pairs. The largest controlled mosaic completed thus far completed has 24 NAC pairs.

Radiometric, geometric, and photometric processing are done with the USGS Integrated Software for Imagers and Spectrometers (ISIS) [5]. The raw images (Experimental Data Records or “EDRs”) are first radiometrically calibrated to radiance factor (or I/F) and pointing and position information is added to the labels using the NAIF SPICE system [6]. The image footprints are then viewed using the ISIS command *qmos* to check and make sure all the images of the controlled mosaic overlap. If they do not all overlap into a single image group, then the multiple image groups are each made into their own controlled mosaic. The overlapping images are seeded with points and registered using ISIS commands *autoseed* and *pointreg*, respectively. *Pointreg* generates the point registration file. Then, ten ground control points are added in an ISIS program, *qnet*. Ground control points are points that tie the images for a mosaic to a ground control, either a DTM, an existing controlled mosaic or a NAC pair with LOLA SPKs projected onto the WAC GLD100 global shape model (100 meter pixel scale). After which, the images for the mosaic are bundle adjusted using the ISIS command *jigsaw.* The output of jigsaw is the bundle output which is used in the next steps. The parameters used for the bundle adjustment are: *observation=no*, which allows each image to be treated as a separate observation instead of all of them being treated as one; *method=sparse*, which solves for a matrix with speed and little memory usage; *twist=no*, which prevents a twist angle being added to the bundle output; *outlier_rejection=yes*, which allows outliers to be found and rejected; *camsolve=all*, so that the coefficients for angles, velocities, and acceleration are solved for the camera angles and is more accurate with all coefficients solved for; *spsolve=position*, solves for the position of the spacecraft; the *spacecraft_position_sigma* is given the value, *300*; and both the *camera_angles_sigma* and *camera_angular_velocity_sigma* are given the values of *0.1*. If the jigsaw bundle output is good, determined by the *Sigma0* value given in the bundle output (which ideally would be around *1.0)* then the images are map projected and mosaicked together.

Geometric Seam Checking: Once the images are mosaicked together, the seams (where two different NAC pairs overlap) are checked at full scale to ensure proper image alignment. Most mosaics have slight seam errors; if they are off by less than 7 or 8 pixels (usually due to uncorrected topography), the mosaic is declared completed. If there are areas where the seam is off by more than 7 or 8 pixels, additional tie points will be added to the unprojected images to help improve image alignment. In some cases seams are mismatched by more than 20 pixels. For these cases the unsatisfactory *pointreg* fit is re-run with a larger matching search chip, or edits to the point registration file are made. When editing the registration file, points with high RMS values from the jigsaw bundle output are removed and new points are added to fill in along the seam to force the images to line up. This process is repeated and until the seams are less than 8 pixels off.

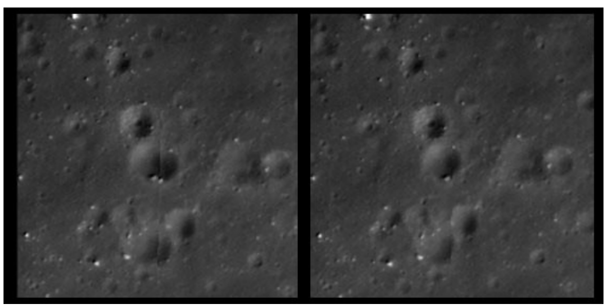

Figure 2: Left image shows an uncontrolled mosaic seam, right image shows the controlled mosaic seam.

Once the geometric seams are finalized, the unprojected images are photometrically corrected (ISIS *photomet*), projected, and mosaicked. Occasionally, *photomet* does not correct or completely remove radiometric offsets, in which case a histogram normalization is performed by interactively displaying the overlapping photometrically corrected radiometrically calibrated images with SPICE information. Using the histogram tool, a box is drawn on regions of overlap with the greatest radiometric mismatches. One NAC pair is chosen as the base pair to match all the images in the mosaic. Each NAC pair is normalized to the base pair working outward from the base pair. For images that do not overlap the base pair the closest normalized image is used.

Error Analysis: The most common causes of geometric errors between NAC pairs are large changes in topography unresolved in the GLD100, and auto registration errors caused by large differences in lighting conditions amongst NAC pairs. When one or both of these conditions occur, *pointreg* has a difficult time matching points in the overlapping areas of the images The bundle output can also have a difficult time registering and matching the points. The jigsaw bundle adjustment output provides RMS values for each point, allowing identification of the largests area of seam offset.

Accuracy: Mosaics are controlled to two different types of ground truth: DTM or a NAC image/pair of NAC images with the necessary LOLA SPKs. Camera orientation can be further refined if the images contain equipment from a US or Soviet lunar mission for which accurate coordinates are known, the camera orientation is updated with these accurate ground truth points (ISIS *deltack*).

Scientific Application: The high resolution and accurate ground representation afforded by controlled NAC mosaics facilitate photogeologic interpretations. The seamless coverage and consistent lighting conditions of FMs over a large ground area makes controlled NAC mosaics an excellent data source for the construction of geologic maps. The applied map projection and precise geodetic control allow morphometric and geographic determinations to within ± 15 meters and aid in the interpretation of geologic units and contacts, as well as the location and environment of spacecraft componetnts left on the lunar surface (Apollo, Luna, Chang'e) . Currently there are 43 LROC NAC controlled mosaics are available on the LROC PDS archive webpage:

http://wms.lroc.asu.edu/lroc/rdr_product_select

References: 1] Robinson, M.S. et al. (2010) *Space Sci. Rev. 150*(1), 81-124. [2] Burns, K.N. et al. (2012) LSPRS XXII, 483-488. [3] Smith, D.E. et al. (2010) *Geophys. Res. Letters,* 37(18), L18204. [4] Scholten, F. et al. (2012) *J. of Geophys. Res. 117,* E00H17. [5] Anderson, J.A. et al. (2004) LPSC XXXV, Abstract #2039. [6] Acton, C.H. Jr. (1996) *Planetary and Space Sci. Vol.* 44 Iss. 1 65-70.